Habitat-specific differences in adaptation to light in freshwater diatoms

Pengling Shi · Hong Shen · Wenjing Wang · Qiang Yang · Ping Xie

Abstract The growth and physiological characteristics of eight strains of diatoms isolated from aquatic habitats with differing water column characteristics were studied under varying light intensities to compare adaptations to low and high light intensity. Diatoms isolated from different habitats were grouped into low light-adapted (LLA) and high light-adapted (HLA) diatoms based on their differences in growth and photoacclimation characteristics. LLA diatoms had higher growth rates and higher photosynthetic activity at relatively lower light intensities (2, 12.5, and 25 μmol photons m^{-2} s^{-1}) compared to relatively higher light intensities (60 and 80 μmol photons m^{-2} s^{-1}). HLA diatoms had higher growth rates and higher photosynthetic activity at relatively higher light intensities (60 and 80 μmol photons m^{-2} s^{-1}) compared to relatively lower light intensities (2, 12.5 and 25 μmol photons m^{-2} s^{-1}). LLA diatoms responded to high light by enhancing non-photochemical quenching (NPQ) while HLA diatoms responded to low light mainly by increasing chlorophyll *a* content. Habitat-specific differences in adaptation to light in diatoms led to differences in light intensity for the formation of diatom blooms in low-light ecosystems and high-light ecosystems. Based on the results of this study, we suggest that the adaptability of diatoms to local habitat conditions should be considered in order to understand the photosynthetic characteristics of these diatom species.

Introduction

Diatom blooms are observed in aquatic ecosystems worldwide and cause serious environmental problems (e.g., Hijnen et al. 2007; Leland et al. 2001). Many studies have focused on the role of environmental factors such as light (Marra and Heinemann 1982), turbulence (Thomas and Gibson 1990), and nutrients (Ferris and Lehman 2007; Sommer 1986) in the dynamics of diatom populations in aquatic ecosystems. Light intensity has been shown to be the main factor controlling the timing of the first occurrence of spring diatom blooms (e.g., Znachor et al. 2013; Letelier et al. 2004) and driving phytoplankton succession during the initial phase of the spring bloom in the north-western Mediterranean Sea (Brunet et al. 2013). Phytoplankton composition is highly related to the light regime of aquatic habitats (Robinson and Rushforth 1987). Light intensity is one of the important factors regulating phytoplankton community structure in Lake Nieuwe Meer, the Netherlands (Huisman et al. 2004). In China's Yanghe Reservoir, light penetration through the water column was considered a major force in affecting phytoplankton morphology during seasonal succession (Su et al. 2014).

The selective role of light on the distribution of phytoplankton communities mainly induces the capacity of light adaptation in each species. Other studies have shown that photosynthetic and growth rate in many phytoplankton species can be affected by light conditions (Dimier et al. 2009; van Leeuwe et al. 2005; van de Poll et al. 2007). Some diatom species adapted to high light intensities showed high growth rates (Wang et al. 2013), high photosynthesis rates, high light

P. Shi
College of Fisheries, Huazhong Agricultural University,
Wuhan 430070, People's Republic of China

P. Shi · H. Shen (✉) · W. Wang · Q. Yang · P. Xie (✉)
Donghu Experimental Station of Lake Ecosystems, State Key Laboratory of Freshwater Ecology and Biotechnology, Institute of Hydrobiology, Chinese Academy of Sciences, Wuhan 430072, People's Republic of China
e-mail: hongshen@ihb.ac.cn
e-mail: xieping@ihb.ac.cn

saturation intensities (Cheah et al. 2013), and efficient responses to photoinhibition (Stamenkovic and Hanelt 2013) under high light regimes. Phytoplankton from a low-light lake (Grande Lake) were better adapted to a low-light environment in winter with higher maximum photosynthetic rates than plankton from a high-light lake (a relict oxbow lake) (Rodríguez et al. 2012), and phytoplankton from low-light sites had lower concentrations of cellular xanthophyll-cycling pigments than phytoplankton from high-light sites (Polimene et al. 2014). The Chl*a* content which can reflect the photoacclimation status was high in low light and low in high light (Brunet et al 2011). Dimier et al. (2009) studied the xanthophyll cycle in six marine phytoplanktonic species and found that the high light-adapted species presented both a low quantity and diversity of photosynthetic accessory pigments and a high pool of xanthophyll-cycling pigments per cell compared to the low light-adapted species. Barnett et al. (2014) suggested that a balance between the physiological and behavioral photoprotective responses existed in intertidal marine diatoms and NPQ is clearly more efficient in non-motile epipsammon than motile epipsammon species.

However, the mechanisms which result in differences in photosynthetic adaptation to light intensity remain unclear. In this study, we hypothesized that diatoms from different light regimes would develop their specific photoacclimation characteristics and physiological characteristics in response to the light regime at a smaller, more local scale. To evaluate the adaptability of diatoms to light regime (low light and high light intensity), we isolated eight strains of diatoms from two high-light habitats (light intensity at a 0.5-m depth greater than 300 μmol photons m^{-2} s^{-1} in spring) and a low-light habitat (light intensity at a 0.5-m depth less than 100 μmol photons m^{-2} s^{-1} in spring) and compared diatom growth rates and chlorophyll fluorescence parameters under five light intensities (2 to 80 μmol photons m^{-2} s^{-1}). We attempted to explore (1) the light-adaptive characteristics of low light-adapted (LLA) and high light-adapted (HLA) diatoms under various light intensities and (2) the physiological regulation of LLA and HLA diatom response to light stress. The results from this study will further our understanding of acclimation to the light regime and physiological strategies in response to light stress in these diatom species.

Six diatom species were cultured in this study: *Stephanodiscus hantzschii*, *Fragilaria crotonensis*, *Nitzschia palea*, *Synedra ulna*, *Stephanodiscus parvus*, and *Synedra acus*, and two *Cyclotella meneghiniana* strains were used in this study, which represent a wide range of diversity in terms of cell sizes and taxa (Table 1). These diatoms are either nanophytoplankton (2 to 20 μm) or microphytoplankton (20 to 200 μm) based on cell size. *S. hantzschii*, a non-motile species, is common in rivers (Kim et al. 2007; Wang et al. 2012); the distribution of *S. hantzschii* is mainly influenced by water column turbulence (Yang et al 2011).

C. meneghiniana is often a dominant species in relatively calm water conditions (Qi et al 2012; Zeng et al. 2007) and is considered as a large niche breadth species (Wang et al 2010). *S. parvus* is found in many temperate lakes at low to modest relative abundance (Sokal 2007). *N. palea* is considered a highly adaptable species regarding light regime (Rodríguez and Pizarro 2007). *F. crotonensis*, *S. aulna*, and *S. acus* are also regarded as highly flexible to light intensity (Bouvy et al. 2006; Schmitt and Nixdorf 1999; Tuji 2000).

Materials and methods

We isolated eight strains (Table 1) of diatoms from three different habitats where diatom blooms have been frequently occurring. The diatoms were divided into two groups (high light-adapted (HLA) diatoms and low light-adapted (LLA) diatoms) according to the results of preliminary experiments. These experiments cultured diatoms at eight light intensities (2 to 300 μmol photons m^{-2} s^{-1}) and found that diatoms from the Hanjiang River had high growth rates and high photosynthetic activities at light intensities lower than 25 μmol photons m^{-2} s^{-1} but showed photoinhibition at 80 μmol photons m^{-2} s^{-1}. Diatoms from Lake Taihu and Guanqiao Pool showed light-limited growth rates at 2 μmol photons m^{-2} s^{-1}, but their growth rates increased with increasing light intensities. According to the response of growth and chlorophyll *a* fluorescence parameters to light stresses in diatoms from different habitats, diatoms from Hangjaing River were defined as LLA diatoms and diatoms from Lake Taihu and Guanqiao Pool were defined as HLA diatoms.

During spring, *S. hantzschii* was the dominant species in the Hanjiang River (85 μmol photons m^{-2} s^{-1} at a 0.5-m depth) while *C. meneghiniana* was the dominant species in Lake Taihu (564 μmol photons m^{-2} s^{-1} at a 0.5-m depth) and Guanqiao Pool (485 μmol photons m^{-2} s^{-1} at a 0.5-m depth). The light intensity in Lake Taihu was estimated from an equation determined from long-term monitoring at the Lake Taihu Ecological Experiment Station (Zhang et al. 2004). Light intensity at Guanqiao Pool and Hanjiang River was measured by using an illuminometer (model wi97178, Ruida, China) in the spring of 2010. Sub-dominant species found in the Hanjiang River were *F. crotonensis*, *N. palea*, and *S. ulna.* In Lake Taihu, the dominant diatoms were *S. parvus* and *S. acus*. The Hanjiang River watershed includes some mountainous areas and receives a large amount of snowmelt from these areas in early spring. During this time, the Hanjiang River flows fast and turbid, and the range of measured discharge was 800 to 8000 m^3 s^{-1} in 2010 (Yang et al. 2012). In Gonghu Bay (Lake Taihu), the average Secchi depth was 117 cm in the spring of 2010 (Qi et al. 2012).

Diatoms were isolated according to standard phycological methods (Stein and Hellebust 1979). Monoclonal diatoms of

Table 1 Information of diatoms used in this study

Species	Taxa	Sampling sites	Sampling year	Average biovolume (μm^3)
Stephanodiscus hantzschii	Centric	Hanjiang River	2010	930.14
Fragilaria crotonensis	Araphid	Hanjiang River	2008	1558.59
Synedra ulna	Araphid	Hanjiang River	2010	2186.61
Nitzschia palea	Raphid	Hanjiang River	2008	1058.28
Cyclotella meneghiniana(T)	Centric	Lake Taihu	2010	144.32
Stephanodiscus parvus	Centric	Lake Taihu	2010	179.713
Synedra acus	Araphid	Lake Taihu	2010	2161.03
Cyclotella meneghiniana(G)	Centric	Guanqiao Pool	2007	289.82

Cyclotella meneghiniana(T) represents *Cyclotella meneghiniana* isolated from Lake Taihu; *Cyclotella meneghiniana*(G) represents *Cyclotella meneghiniana* isolated from Guanqiao Pool

each strain were cultured in D1 medium (Zhang and Huang 1991). Concentrated diatom cells were cleaned using H_2SO_4 and observed under scanning electron microscope (SEM, JSM-6390LV, Japan) (Zhang and Huang 1991). Identification of algal species was based on the shape and pattern of the surface of the diatom shell (Hu and Wei 2006).

Growth experiments were conducted in illuminated incubators with a 14/10 light/dark cycle and 18 °C/16 °C temperature regimes. The light intensity was 2, 12.5, 25, 60, and 80 μmol photons m^{-2} s^{-1} with cool-white fluorescent light. The 80 μmol photons m^{-2} s^{-1} was the highest light treatment in the present experiment because 80 μmol photons m^{-2} s^{-1} was high enough to cause varying degrees of photoinhibition in all LLA diatoms in our preliminary experiment. Each 250-mL flask contained 200-mL culture at an initial algae concentration of about $5 \times 10^7 \pm 1.5 \times 10^6$ cells L^{-1}. Triplicate cultures were used for each treatment. All cultures were regularly shaken two times per day to prevent diatoms from adhering to flasks. In order to eliminate the effects of nutrient depletion on the growth and physiological characteristics of diatoms, all the cultures were transferred weekly to fresh D1 medium. The experiment lasted 16 days. Samples were harvested every second day to monitor cell density and photosynthetic parameters. The results are given as the average value among the replicates with the standard deviation.

Growth rates

Diatom cells preserved with 1 % Lugol's iodine solution were counted using counting chambers under an Olympus CX21 light microscope. The specific growth rate of each strain was calculated using Eq. (1):

$$\mu = [\ln B_{t2} - \ln B_{t1}] / \Delta t \qquad (1)$$

Where μ is the specific growth rate (day^{-1}), B_{t1} is the initial cell density; B_{t2} is the cell density on the last day of the logarithmic growth phase.

Chlorophyll *a* (Chl*a*) concentration

Chlorophyll *a* concentration was measured using the spectrophotometric method (Stein and Hellebust 1979). A 5-mL sample was collected from each treatment and concentrated by centrifugation at $100 \times g$ for 10 min. Then the concentrates were dissolved in 5-mL 90 % acetone and kept in the dark at 4 °C overnight for Chl*a* extraction. The Chl*a* concentrations were determined from absorbance at 665, 645, and 630 nm with a spectrophotometer (Stein and Hellebust 1979) (Shimadzu UV2550, Japan).

$$\text{Chl}a\left(\text{mg L}^{-1}\right) = 11.6 \, \text{OD}_{665} - 1.31 \, \text{OD}_{645} - 0.14 \, \text{OD}_{630} \qquad (2)$$

Chlorophyll *a* are expressed as pg Chl*a* per microgram of carbon (pg Chl*a* μg^{-1} C). The carbon content of each strain was estimated by using biovolume (Warnaars and Hondzo 2006): $\log_{10} C = 0.758 \log_{10} V - 0.422$ (for diatoms), where C is cell carbon in micrograms and V is cell volume in μm^3.

Chlorophyll *a* fluorescence parameters

Photosynthetic performance was measured using a pulse amplitude-modulated fluorescence monitoring system (Phyto-PAM, Walz, Germany). Subsamples of each culture were transferred to quartz glass cuvettes and positioned in the detector system. The actinic light level and saturating pulse level were set at 264 μmol photons m^{-2} s^{-1} at a length of 180 s and 4000 μmol photons m^{-2} s^{-1} at a length of 500 ms, respectively.

The effective photochemical efficiency The effective quantum yield of PS II ($\Delta F/F'_m$, Y) was measured using the quenching method (Schreiber et al. 1994). Values of $\Delta F/F'_m$ were calculated based on Eq. (3).

$$\Delta F/F'_m = [F'_m - F_s] / F'_m \qquad (3)$$

Where F_s is the fluorescence at actinic light, F'_m is the maximum fluorescence after saturating light pulses. $\Delta F/F'_m$ describes the actual quantum yield of photochemical conversion of excitons already migrating in the light-harvesting complex of PSII (Hartig et al. 1998).

Non-photochemical quenching (NPQ). NPQ is a sensitive parameter to assess excess heat dissipation in algae (Lavaud et al. 2004). NPQ was calculated by Eq. (4) (Kashino et al. 2002).

$$NPQ = (F_m - F'_m)/F'_m \qquad (4)$$

Where F_m is the maximum fluorescence yield following dark adaptation of 15 min, and F'_m is the maximum fluorescence yield of light-adapted sample.

Rapid light response curve (RLC). RLCs were used to demonstrate the relative change of photosynthetic performance under different light intensities (Ihnkena et al. 2010). Each sample was exposed to each of 12 increasing actinic light levels for 10 s (from 3 to 1480 µmol photons m^{-2} s^{-1}), and the r*ETR* vs PAR curve (RLC) was plotted using the model of Platt et al. (1980) to obtain photosynthetic parameters (α, r*ETR*$_{max}$, I_k) by the least-squares method.

$$rETR = rETR_{max} \cdot \left(1 - e^{-\alpha \cdot PAR/Pm}\right) \cdot e^{-\beta \cdot PAR/Pm} \qquad (5)$$

where α is the initial slope of RLC and reflects the photon-capturing efficiency under light-limiting conditions. The r*ETR*$_{max}$ represents maximum relative electron transport rate of the RLC (Genty et al. 1989). Effects on r*ETR*$_{max}$ are in components of the photosynthetic electron transport chain (Behrenfeld et al. 2004; MacIntyre et al. 2002) and attributed to changes in Calvin cycle enzyme (RUBISCO) concentration and activity.

$$I_k = rETR_{max}/\alpha \qquad (6)$$

The light saturation point of photosynthesis (I_k) indicates the PAR at which photosynthesis is saturated.

Cell ultrastructure

Samples (50 mL) of algal culture were collected under sterile conditions after a 5-h light exposure under low (LL, 2 µmol photons m^{-2} s^{-1}), medium (ML, 25 µmol photons m^{-2} s^{-1}), and high (HL, 80 µmol photons m^{-2} s^{-1}) light intensities. Triplicate cultures were used for each treatment. Medium light intensity was used as control. Each sample was centrifuged at $50 \times g$ for 6 min under 4 °C. The pellet was suspended in 2.5 % glutaraldehyde and kept at 4 °C overnight and then washed

with 0.1 M phosphate buffer (pH 7.4). After post-fixation in 1 % osmium tetroxide for 2 h at 20 °C, the samples were dehydrated by serial transfers through a progressive aqueous–acetone series (30–100 %) and embedded in Spurr's resin. Sections were cut and subsequently stained with uranyl acetate (Stempak and Ward 1964) followed by lead citrate. Sections were viewed by transmission electron microscopy (TEM, Hitachi H-7650) operating at 80 kV. From each sampling, 10 TEM micrographs were examined. All quantitative analyses were made on sections through the cell equator.

Statistical analysis

Origin 8.0 (Microcal Software, USA) was used for graphical analyses, and SPSS 16.0 (Windows Software, Inc., USA) was used for statistical analyses. Differences in growth rate, Chl*a* content, and RLC parameters were compared using one-way ANOVA followed by Tukey post-hoc tests. Results were considered statistically significant using α-level of 0.05.

Results

Growth of diatoms

The average growth rate of LLA diatoms (0.034 ± 0.005 day^{-1}) was significantly higher than that of HLA diatoms (0.010 ± 0.002 day^{-1}) although all eight diatoms showed low growth rates at a light intensity of 2 µmol photons m^{-2} s^{-1} (Fig. 2c). The cell number of *F. crotonensis* and *S. ulna* showed a slight decrease on day 3 but recovered rapidly from day 5 (Fig. 1a). There was no obvious decrease in *S. hantzschii* and *N. palea* on day 3. The cell densities of all four HLA diatoms decreased on day 3 but increased during the later growth phase. Differences of growth rates were found between LLA and HLA diatoms at light intensity of 12.5 µmol photons m^{-2} s^{-1} (Fig. 1b). The average growth rate of LLA diatoms was 0.128 ± 0.023 day^{-1} (Fig. 2c), and *S. hantzschii* showed relatively high growth rate at 12.5 µmol photons m^{-2} s^{-1} (Fig. 2a). The cell density of HLA diatoms increased slightly, and no obvious decrease was found on day 3 at 12.5 µmol photons m^{-2} s^{-1}. At 25 µmol photons m^{-2} s^{-1} (Fig. 1c, Fig. 2a), the growth rates of LLA diatoms were still higher than those of HLA diatoms and *S. hantzschii* was also the highest one. The average growth rate in LLA diatoms was 2.09 and 1.66 times that of HLA diatoms at 12.5 µmol photons m^{-2} s^{-1} ($F=16.672$, $P=0.006$) and 25 µmol photons m^{-2} s^{-1} ($F=9.912$, $P=0.020$), respectively (Fig. 2c).

The cell density of HLA diatoms grew fast with increasing light intensities. The average growth rate of HLA diatoms exceeded that of LLA diatoms at 60 µmol photons m^{-2} s^{-1} (Fig. 1d, Fig. 2c). The cell density of *C. meneghiniana*(T) exceeded *S. hantzschii* on day 3. The cell density of *S. parvus*
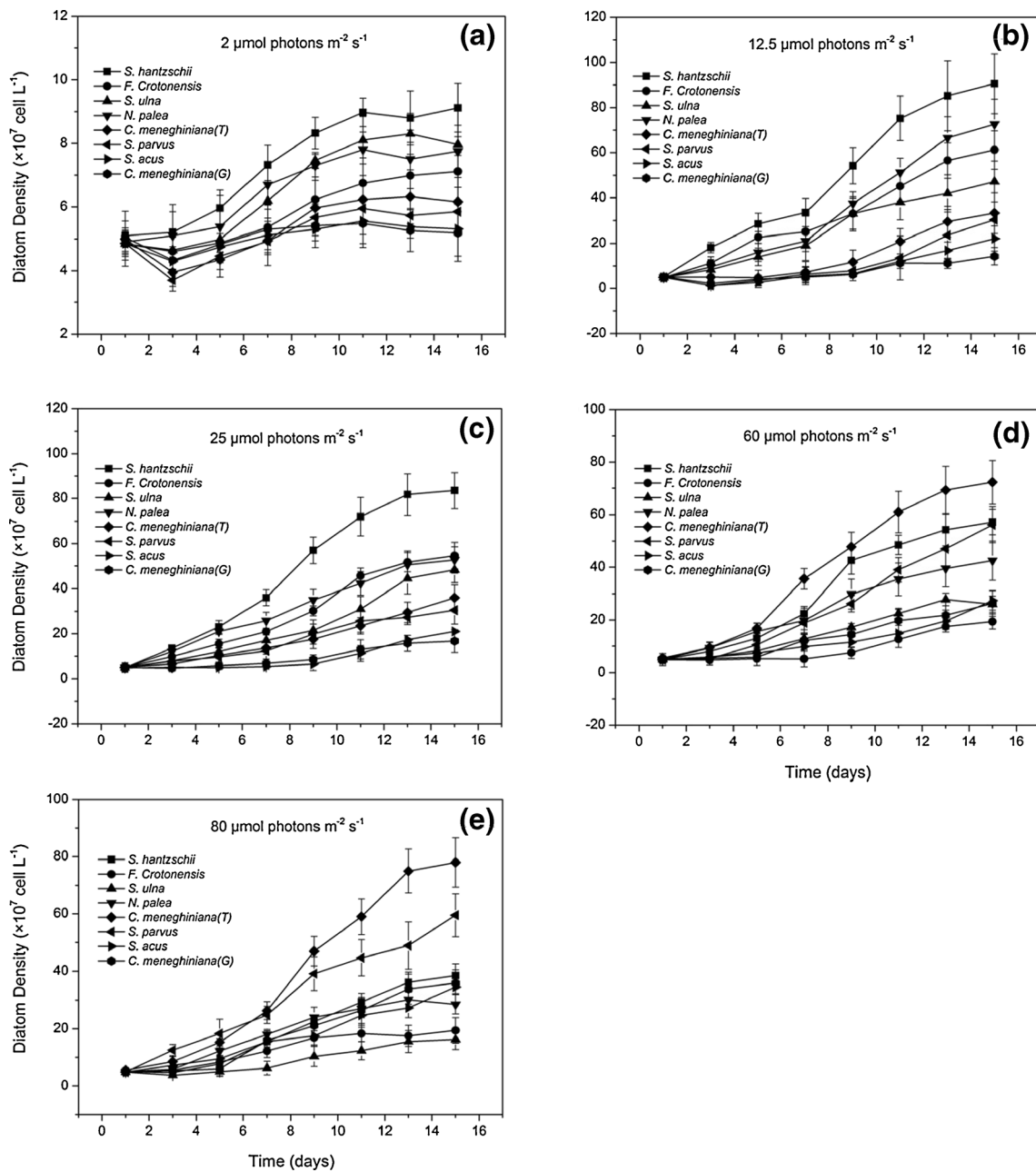
Fig. 1 Growth curves of eight diatoms at five light intensities. Data are means±standard deviations $n=3$

exceeded *N. palea* on day 11. At a light intensity of 80 μmol photons m^{-2} s^{-1} (Fig. 1e), HLA diatoms had high growth (Fig. 2c) and *C. meneghiniana*(T) showed the highest growth rate while LLA diatoms grew slowly (Fig. 2b). The average growth rate in HLA diatoms was 1.45 and 1.69 times that of the LLA diatoms at 60 μmol photons m^{-2} s^{-1} ($F=8.871$, $P=$ 0.025) and 80 μmol photons m^{-2} s^{-1} ($F=8.181$, $P=0.029$), respectively (Fig. 2c).

LLA and HLA diatoms showed distinct patterns of growth rate under various light intensities. LLA diatoms had their maximum specific growth rates at 12.5 or 25 μmol photons m^{-2} s^{-1} but exhibited a decreasing trend above

25 μmol photons m^{-2} s^{-1} (Fig. 2a). The maximum specific growth rates of HLA diatoms occurred at 60 or 80 μmol photons m^{-2} s^{-1} (Fig. 2b).

Chlorophyll *a* content

We did not find any significant differences in Chl*a* content in LLA diatoms between LL and HL treatments (Fig. 3a). Chl*a* contents at LL (Chl*a*$_{LL}$) of *S. hantzschii* were higher than Chl*a* contents at HL (Chl*a*$_{HL}$) during the first 3 days. Chl*a*$_{HL}$ exceeded Chl*a*$_{LL}$ and showed a slight increase since day 5. Chl*a*$_{HL}$ and Chl*a*$_{LL}$ in *F. crotonensis* were similar during the

Fig. 2 Specific growth rates of LLA and HLA diatoms under five light intensities. Data are means± standard deviations of specific growth rates, $n=3$. **a** Specific growth rates in four LLA diatoms. **b** Specific growth rates in four HLA diatoms. **c** The average values of specific growth rates in LLA and HLA diatoms. *Asterisks* show statistical significance with $P<0.05$ (*) and $P<0.01$ (**)
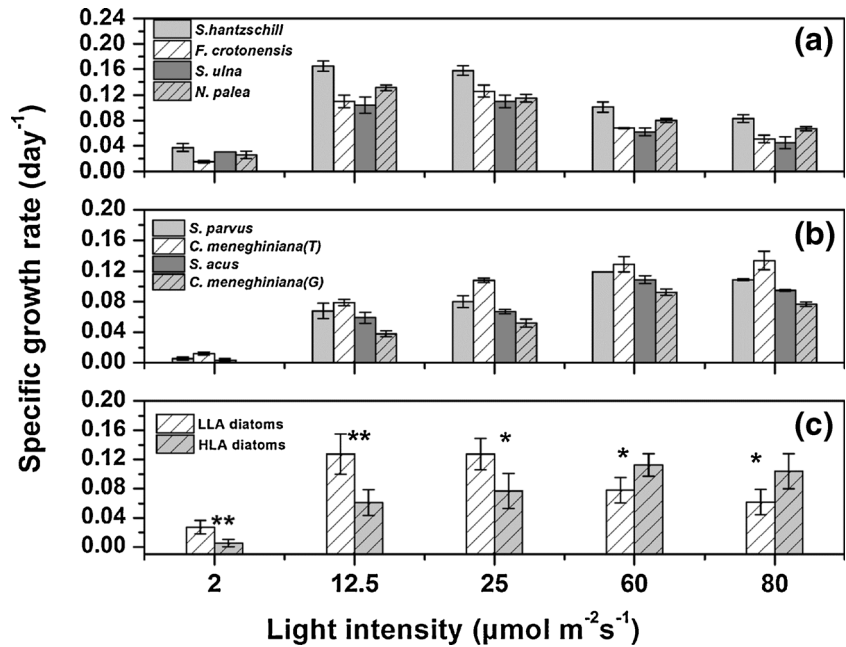

first 5 days but exceeded $Chla_{LL}$ from day 7. $Chla_{HL}$ of *N. palea* was higher than $Chla_{LL}$ during the whole growth period. No significant differences were found in $Chla_{LL}$ and $Chla_{HL}$ of *N. palea*. $Chla_{LL}$ fluctuation was found in all HLA diatoms (Fig. 3b).A significant increase in Chl*a* content at LL on day 3 was found in *C. meneghiniana*(T) and *S. acus* ($P<0.01$), followed by *S. parvus* and *C. meneghiniana*(G) ($P<0.05$). $Chla_{LL}$ of *C. meneghiniana*(T) increased dramatically from day 3 and reached the maximum value on day 7 which was about two times as high as $Chla_{HL}$ in *C. meneghiniana*(T). Chl*a* contents of *S. parvus* showed an obvious increase at LL from day 3 to day 7 but only a slight increase at HL. The ratios of Chl*a* content at LL to Chl*a* content at HL of *S. acus* were close to 2, which lasted from day 3 to day 7, but $Chla_{HL}$ was greater than $Chla_{LL}$ from day 11. $Chla_{LL}$ of *C. meneghiniana*(G) increased rapidly from day 3 to day 9 but started to decline from day 9.

Ultrastructure

Light intensity affected cell ultrastructure (Fig. 4). Sectioned chloroplast areas of *S. hantzschii* and *C. meneghiniana*(T) were 25±3 % and 34±4 %, respectively, for the ML (Fig. 4b, e). For *C. meneghiniana*(T), chloroplasts were the dominating organelles, comprising 43±7 % of the sectioned area of cells at LL (Fig. 4d), while there was no distinct difference in sectioned chloroplast areas under HL treatment (32 ±5 %) (Fig. 4f) compared to ML treatment (Fig. 4e). For *S. hantzschii*, the sectioned chloroplast areas were 28±4 % and 17.5±3 % under LL and HL treatment, respectively (Fig. 4a, c).
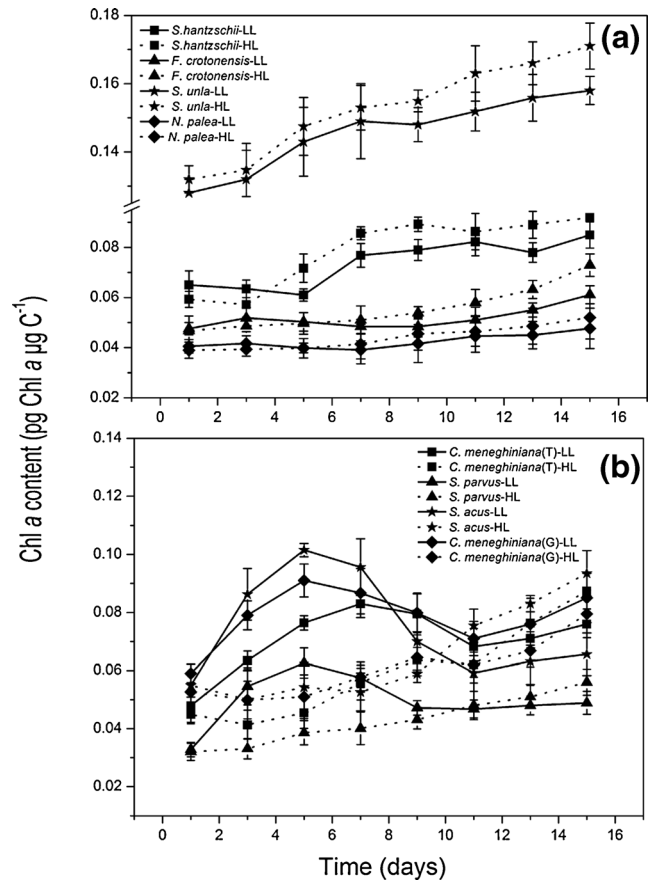
Fig. 3 Change of chlorophyll *a* content in LLA and HLA diatoms at LL and HL. Data are means±standard deviations of the Chl *a* content, $n=3$. *LL* low light intensity (2 μmol photons m^{-2} s^{-1}), *HL* high light intensity (80 μmol photons m^{-2} s^{-1})
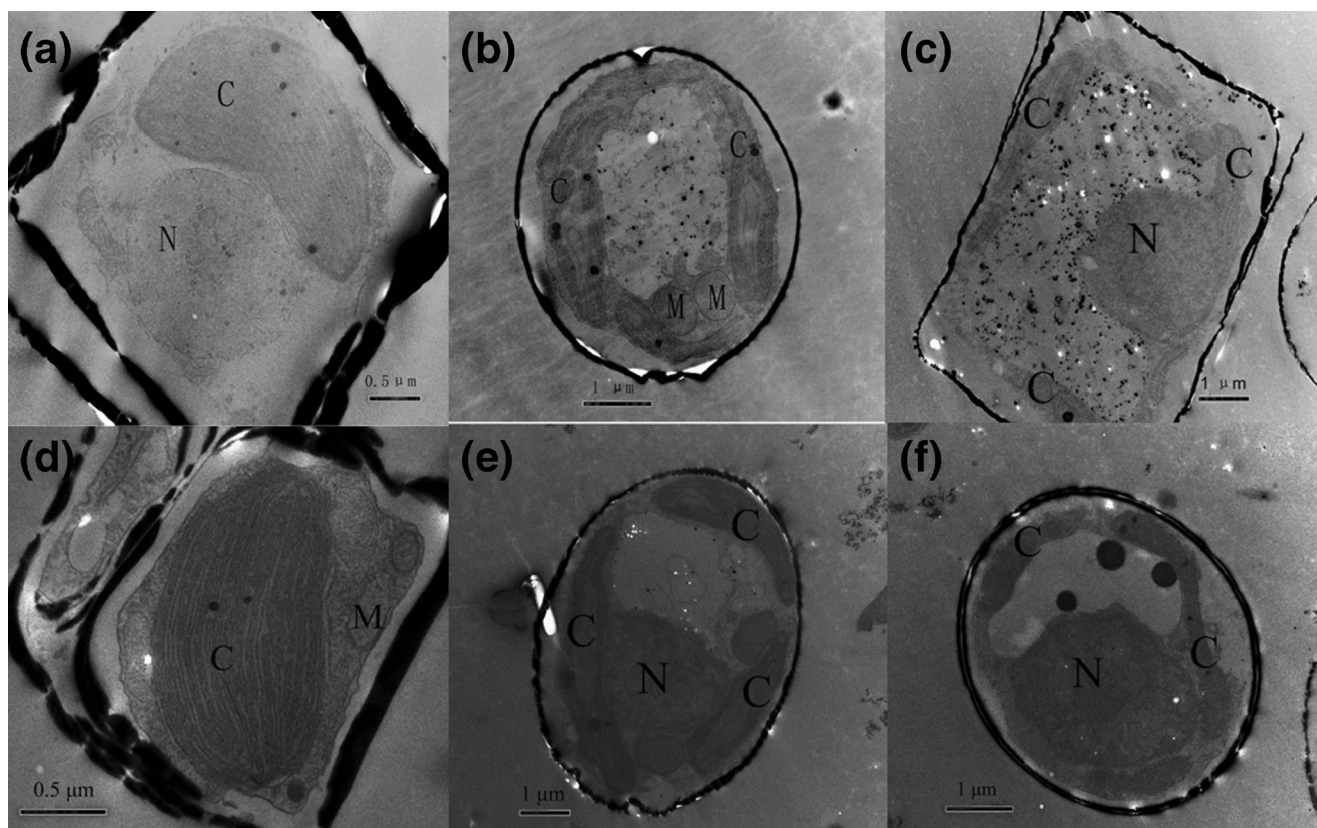
Fig. 4 Ultrastructure of *S. hantzschii* and *C. menegihiniana*(T). **a** *S. hantzschii* cells at LL, **b** *S. hantzschii* cells at ML, **c** *S. hantzschii* cells at HL, **d** *C. meneghiniana*(T) cells at LL, **e** *C. meneghiniana*(T) cells at ML, **f** *C. Meneghiniana*(T) cells at HL. *C* chloroplast, *N* nucleus, *M* mitochondrion. *Scale bar* was 0.5 μm in **a** and **d** and 1 μm in **b**, **c**, **e**, and **f**. LL=2 μmol photons m^{-2} s^{-1}; ML=25 μmol photons m^{-2} s^{-1}; HL=80 μmol photons m^{-2} s^{-1}

Effective quantum yield of PS II

The $\Delta F/F'_m$ values decreased gradually with increasing light levels and was lowest at 80 μmol photons m^{-2} s^{-1} in *S. hantzschii* (Fig. 5a). The maximum $\Delta F/F'_m$ value of the LLA diatom *S. hantzschii* was 0.573 and occurred at 2 μmol photons m^{-2} s^{-1} on day 7. The $\Delta F/F'_m$ values of *S. hantzschii* at 12.5 μmol photons m^{-2} s^{-1} were close to $\Delta F/F'_m$ values at 2 μmol photons m^{-2} s^{-1}. The $\Delta F/F'_m$ values of *S. hantzschii* at 60 and 80 μmol photons m^{-2} s^{-1} decreased gradually from day 9. The $\Delta F/F'_m$ values of *F. crotonensis* increased from day 3 and reached the maximum value at 25 μmol photons m^{-2} s^{-1} on day 7, followed by the $\Delta F/F'_m$ values at 12.5 and 2 μmol photons m^{-2} s^{-1} (Fig. 5b). The $\Delta F/F'_m$ of *F. crotonensis* at 60 and 80 μmol photons m^{-2} s^{-1} decreased after day 7. Same as *F. crotonensis*, *S. unla* reached the maximum $\Delta F/F'_m$ at 25 μmol photons m^{-2} s^{-1}, followed by 12.5 and 2 μmol photons m^{-2} s^{-1} (Fig. 5c). The $\Delta F/F'_m$ of *N. palea* at 12.5 and 25 μmol photons m^{-2} s^{-1} increased slowly and reached a maximum on day 13, followed by the $\Delta F/F'_m$ at 2, 60, and 80 μmol photons m^{-2} s^{-1}, which decreased slightly in the later stage (Fig. 5d).

The $\Delta F/F'_m$ of *C. meneghiniana*(T) increased from day 3 at all light intensities except 2 μmol photons m^{-2} s^{-1} (Fig. 5e). The $\Delta F/F'_m$ of *C. meneghiniana*(T) at 80 μmol photons m^{-2} s^{-1} were higher than at the other four light intensities, while at 2 μmol photons m^{-2} s^{-1} $\Delta F/F'_m$ decreased dramatically from day 7. The maximum $\Delta F/F'_m$ of *S. parvus* (0.612±0.031) was obtained at 60 μmol photons m^{-2} s^{-1} on day 11 (Fig. 5f). The $\Delta F/F'_m$ of *S. parvus* at 80 μmol photons m^{-2} s^{-1} were a little lower than at 60 μmol photons m^{-2} s^{-1}, followed by $\Delta F/F'_m$ values at 25, 12.5, and 2 μmol photons m^{-2} s^{-1}. A slight decrease was found in $\Delta F/F'_m$ of *S. parvus* at 2 μmol photons m^{-2} s^{-1} from day 9. *S. acus* had higher $\Delta F/F'_m$ values at 60 and 80 μmol photons m^{-2} s^{-1} (Fig. 5g). The $\Delta F/F'_m$ of *S. acus* showed a slight decrease at 25 and 12.5 μmol photons m^{-2} s^{-1} from day 11 and a sharp decrease at 2 μmol photons m^{-2} s^{-1} after day 7. *C. meneghiniana*(G) had the maximum $\Delta F/F'_m$ at 60 μmol photons m^{-2} s^{-1} on day 11, followed by 80 μmol photons m^{-2} s^{-1} (Fig. 5h). The decrease in $\Delta F/F'_m$ of *C. meneghiniana*(G) began from day 13 at 12.5 μmol photons m^{-2} s^{-1} and day 9 at 2 μmol photons m^{-2} s^{-1}.

The $\Delta F/F'_m$ of *S. hantzschii* reached the maximum values at 2 μmol photons m^{-2} s^{-1}, and the $\Delta F/F'_m$ of the other 3 LLA diatoms slightly decreased, while that of all four HLA diatoms decreased markedly. At 80 μmol photons m^{-2} s^{-1}, the HLA diatoms reached relatively high $\Delta F/F'_m$, while the LLA diatoms had the lowest $\Delta F/F'_m$.

Fig. 5 $\Delta F/F'_m$ values of eight diatoms under different light intensities during the experiment period. The unit of light intensity is µmol photons m^{-2} s^{-1}. Data are medians±standard deviations of $\Delta F/F'_m$ values, $n=3$


$\Delta F/F'm$
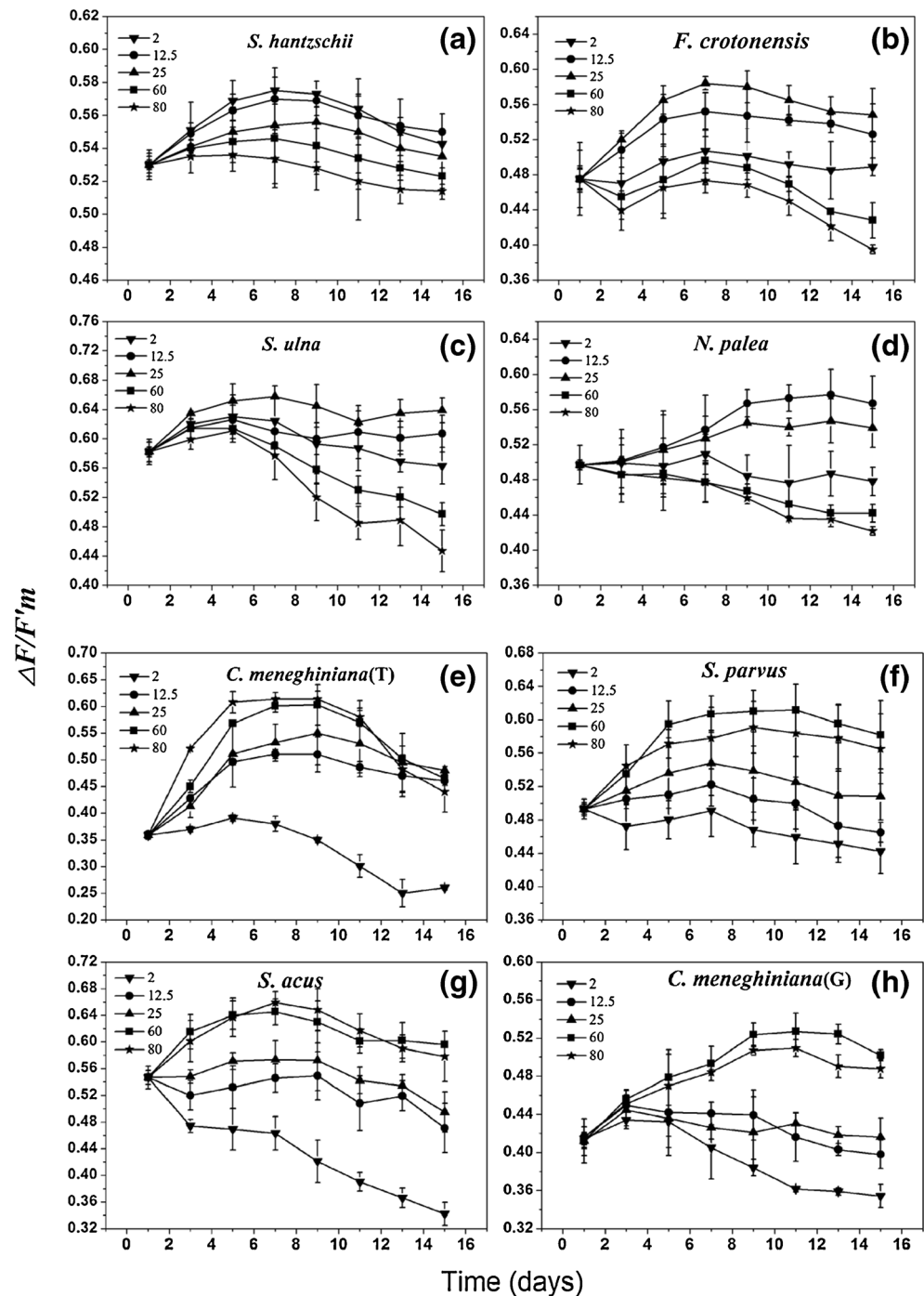
Non-photochemical quenching

Changes of NPQ value in LLA diatoms are shown in Fig. 6a. The NPQ of *S. hantzschii* at HL increased from day 3 and reached a maximum on day 7. A small fluctuation around the original value was found in NPQ at LL. NPQ of *F. crotonensis* at HL increased slightly to a maximum on day 9, while that at LL showed a slight decreasing tendency. NPQ of *S. ulna* and *N. palea* at HL increased from day 3 and decreased below NPQ values at LL on

day 9 and day 11, respectively. The NPQ of HLA diatoms exhibited another trend (Fig. 6b). NPQ of *C. meneghiniana*(T) at HL was lower than NPQ at LL, and the ratio of NPQ at HL to NPQ at LL (NPQ$_{HL}$/NPQ$_{LL}$) was in the range of 0.516~0.774. NPQ of *S. parvus* at HL decreased, and the NPQ$_{HL}$/NPQ$_{LL}$ ratios were lower than 0.5 from day 5. NPQ of *S. acus* at HL dropped in the initial stage and recovered from day 11. No obvious differences were found in NPQ of *C. meneghiniana*(G) between LL and HL, and the NPQ$_{HL}$/NPQ$_{LL}$ was close to 1.
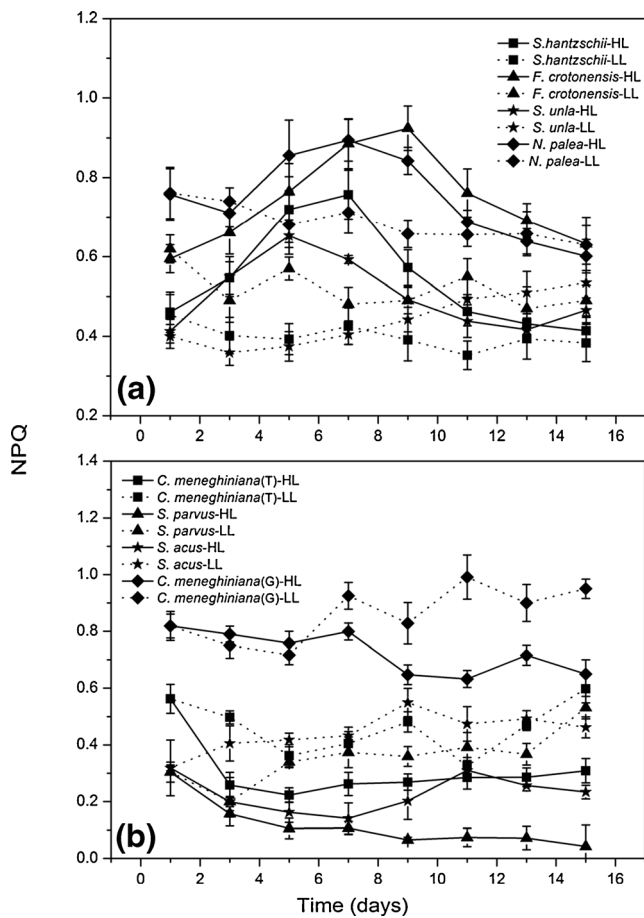
Fig. 6 The NPQ values in LLA and HLA diatoms during the experiment period. Data are means±standard deviations of NPQ values, $n=3$

Rapid light curves

Photosynthetic parameters photon-capturing efficiency (α), maximum electron transport rate (rETR_{max}), and light saturation point (I_k) in lotic and lentic diatoms were compared under low light intensity (LL, 2 µmol photons m^{-2} s^{-1}) and high light intensity (HL, 80 µmol photons m^{-2} s^{-1}). Because intense responses from diatom regulation of Chl$a$ and NPQ were almost found on day 5, we sampled on day 5 and day 13 to compare (Table 2). The α of *S. hantzschii* was the highest one in the LLA diatoms (0.293±0.033 µmol photons m^{-2} s^{-1}) at LL on day 5, followed by *N. palea* (0.2815±0.017 µmol photons m^{-2} s^{-1}), *F. crotonensis* (0.266±0.021 µmol photons m^{-2} s^{-1}), and *S. ulna* (0.227± 0.026 µmol photons m^{-2} s^{-1}). The α values of LLA diatoms at HL were significantly lower than that at LL on day 5. On day 13, the α values of LLA at LL decreased slightly, while the α values of LLA at HL recovered. The rETR_{max} values of *S. hantzschii* at HL were much higher than those at LL day 5, but decreased to near rETR_{max} value at LL on day 13. A similar phenomenon was found in the other three LLA diatoms. The highest I_k value of LLA diatoms at LL was observed in *N. palea* (55.3±4.218 µmol photons m^{-2} s^{-1}). The highest I_k values of the LLA diatoms at HL were significantly higher than those at LL, but dropped on day 13 ($P<0.05$).

On day 5, the α values of *S. parvus* at LL were significantly higher than at HL, followed by *C. meneghiniana*(G), *C. meneghiniana*(T), and *S. acus*. On day 13, the α values of HLA diatoms at LL decreased to near the α values of the HLA

Table 2 Photosynthetic parameters in eight diatoms under low and high light intensities. Data are means±standard deviations, $n=3$

Species	Light treatments	α (µmol photons m^{-2} s^{-1})		rETR_m		I_k (µmol photons m^{-2} s^{-1})	
		Day 5	Day 13	Day 5	Day 13	Day 5	Day 13
S. hantzschii	LL	0.293±0.033	0.282±0.016	102.999±6.321	94.225±2.591	27.2±2.572	25.5±2.345
	HL	0.258±0.031	0.267±0.011	117.157±7.214	97.889±2.341	53.6±3.612	31.5±1.932
F. crotonensis	LL	0.266±0.021	0.2505±0.023	36±4.123	30.36±1.734	32.3±1.834	28.5±1.763
	HL	0.2345±0.025	0.248±0.019	45.75±3.856	32.8±1.563	45.7±2.163	34.5±2.734
S. ulna	LL	0.227±0.026	0.211±0.028	53.65±5.325	51.3±3.452	35.5±3.782	31.2±3.243
	HL	0.1885±0.021	0.2185±0.025	67.55±2.478	57.9±4.235	47.5±4.328	37.3±2.981
N. palea	LL	0.2815±0.017	0.263±0.015	59.7±5.346	51.2±2.131	55.3±4.218	52.7±4.531
	HL	0.248±0.018	0.259±0.016	72.25±4.634	54.45±2.532	71.9±2.372	56.1±3.924
C. meneghiniana[t]	LL	0.259±0.018	0.235±0.027	75.892±3.349	67.557±3.245	143±5.793	158.9±4.633
	HL	0.223±0.027	0.228±0.024	136.934±9.374	140.018±5.321	192±7.349	181.2±5.173
S. parvus	LL	0.2385±0.015	0.183±0.015	69.45±8.347	57.9±3.563	96.9±4.542	103.2±2.653
	HL	0.1865±0.016	0.189±0.011	90.8±6.824	92.6±4.347	110.8±3.893	114±3.187
S. acus	LL	0.249±0.022	0.211±0.012	45.939±5.348	29.13±1.347	128.2±5.642	121.4±3.562
	HL	0.215±0.023	0.203±0.013	84.229±4.231	78.599±3.239	205.1±6.743	196.93±6.347
C. meneghiniana[g]	LL	0.255±0.027	0.227±0.025	54.5±3.437	35.2±1.235	135.2±4.892	148.9±5.127
	HL	0.217±0.015	0.2205±0.017	96.85±2.452	109.6±6.342	171.9±3.981	177±4.832

LL low light intensity (2 µmol photons m^{-2} s^{-1}), *HL* high light intensity (80 µmol photons m^{-2} s^{-1})

diatoms at HL. The $rETR_{max}$ of HLA diatoms at LL were much lower than at HL on day 5, and a small fluctuation was found on day 13. I_k values of HLA diatoms at LL were lower than those at HL on day 5, but increased on day 13.

Discussion

Growth characteristics of LLA and HLA diatoms under different light intensities

Growth rates of LLA diatoms increased with increasing light intensities in a lower range of light intensities (0~25 μmol photons m^{-2} s^{-1}), but decreased above 25 μmol photons m^{-2} s^{-1}, indicating that LLA diatoms were low light adapted. Growth rates of HLA diatoms increased with increasing light intensities (0 to 80 μmol photons m^{-2} s^{-1}) without obvious photoinhibition, and the optimum irradiance for HLA diatoms was much higher than that for LLA diatoms. We assume that HLA diatoms in this study could adapt to much higher light intensities in the field than in the experimental conditions because the light saturation point for growth of HLA diatoms was not reached. The high growth rate of *S. hantzschii* at LL illustrated the superior ability of this species to adapt to low light. A similar pattern was found by Kolmakov et al. (2002). However, a high irradiance of 13 MJ m^{-2} was found when *S. hantzschii* was the dominant diatom in the lower Nakdong River (Kim et al. 2007). Some studies show that *F. crotonensis* was well adapted to a low light environment (e.g., Hartig and Wallen 1986; Harris 1978), and the optimum light intensity to maintain a high growth rate for *F. crotonensis* was 27.6 μmol photons m^{-2} s^{-1} (Rhee and Gotham 1981). However, other studies have found that when *F. crotonensis* was dominant in Lake Erie (USA) and Lake Aydat (France), the light intensity reached up to 95 μmol photons m^{-2} s^{-1} (Hartig and Wallen 1986) and 150 μmol photons m^{-2} s^{-1} (Dauta et al. 1990), respectively. The optimum light intensity for *S. acus* was in the range of 200~300 μmol photons m^{-2} s^{-1} in Lake Melangsee (Schmitt and Nixdorf 1999), but was 63.5 μmol photons m^{-2} s^{-1} in River Spree (Germany) (Köhler 1994). Thus, light-adaptive characteristics associated with local light intensities in the habitat where algae are growing might be important in addition to species-specific characteristics. For example, Kropuenske et al. (2009) found that *Fragilariopsis cylindrus* isolated from a low light regime exhibited low growth rates at higher light intensities from 75 to 125 μmol photons m^{-2} s^{-1}. HLA diatoms (*Skeletonema costatum*, *Thalassiosira weissflogii*, and *Chaetoceros curvisetus*) exhibited significantly lower growth rates under low-light treatment than under high-light treatment in a laboratory experiment (Wang et al. 2013).

Habitat-specific differences in adaptation to light in diatoms lead to differences in light intensity for the formation of diatom blooms in low-light ecosystems and high-light
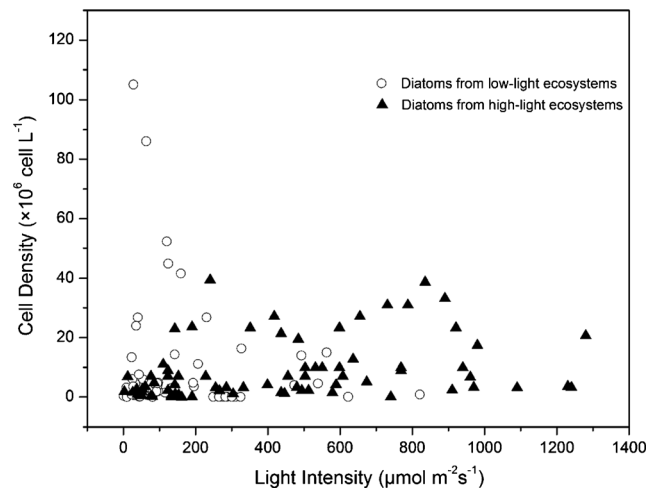
Fig. 7 The relationships between diatom densities and light intensities in the high-light and low-light ecosystems. Light intensity was the light intensity at a 0.5-m depth in water column. Circles and triangles represent data collected from low-light ecosystems and high-light ecosystems, respectively

ecosystems. Summarizing the results from previous surveys (Fig. 7) (e.g.,Gikuma-Njuru et al. 2013; Jaeger et al. 2008; Pannard et al. 2007; Rothenberger et al. 2009), it clearly indicated that there are significant differences in light conditions between high-light ecosystems and low-light ecosystems when diatoms dominate in the water column. Aquatic ecosystems with annual mean light intensity (at a 0.5-m depth) below 300 μmol photons m^{-2} s^{-1} are defined as low-light ecosystems, while above 300 μmol photons m^{-2} s^{-1}, they are defined as high-light ecosystems. When diatom densities were greater than 2×10^7 cells L^{-1}, the light intensity was in the range of 27.7~230.2 μmol photons m^{-2} s^{-1} in low-light ecosystems, while in high-light ecosystems, it was in the range of 142.0~920.4 μmol photons m^{-2} s^{-1}. It suggested that the ideal light intensity for diatom dominance in high-light ecosystems is considerably higher than in low-light ecosystems.

Photoacclimation properties of LLA and HLA diatoms

The effective quantum yield ($\Delta F/F'_m$) is closely related to the CO_2 assimilation rate that can affect the capacity to convert solar energy into organic material, which consequently impacts on the growth of algae (Edwards and Baker 1993). The photosynthetic rate (mg C [mg Chl$a$]$^{-1}$ h^{-1}) is proportional to the effective quantum yield (Hartig et al. 1998). In our study, although the eight diatoms were isolated from field sites in different years, the growth rates and photosynthetic parameters of LLA and HLA diatoms exhibited distinct habitat-specific traits. The $\Delta F/F'_m$ values of the diatoms showed a similar trend as their growth rates. The higher $\Delta F/F'_m$ values of LLA diatoms were accompanied by higher growth rates at light intensities of 12.5 and 25 μmol photons m^{-2} s^{-1}. Under low light conditions, the $\Delta F/F'_m$ values of *S. hantzschii* were higher than for the other 3 LLA diatoms, and it was consisted with the change in growth rate. The obvious

decrease of $\Delta F/F'_m$ values in *F. crotonensis*, *S. ulna*, and *N. palea* during the latter period at 60 and 80 μmol photons m^{-2} s^{-1} reflected the decreasing growth rates in these three LLA diatoms. This was consistent with other LLA species which often exhibit a low light-saturated growth rate and high photosynthetic efficiency (Gameiro et al. 2011). Low light saturation and high photosynthetic efficiency suggest that *S. hantzschii* developed a high tolerance of low light stress, and this physiological characteristic could help *S. hantzschii* outcompete other species in the Hanjiang River where the high tolerance of low light could help it to achieve superiority over other species to form blooms in early spring.

The highest $\Delta F/F'_m$ values of *C. meneghiniana*(T) at 80 μmol photons m^{-2} s^{-1} and that of *C. meneghiniana*(G), *S. parvus*, and *S. acus* at 60 μmol photons m^{-2} s^{-1} correspond to the high growth rates in the HLA diatoms. Different degrees of decline of $\Delta F/F'_m$ values in the four HLA diatoms at LL can explain the low average growth rate of HLA diatoms at LL.

Chl*a* regulation

Light history is considered as a determining factor for the kinetics of pigment variations (Anning et al. 2000). Previous studies have demonstrated that diatoms can regulate their Chl*a* content with light intensity changes (e.g., Migné et al. 2004; Laviale et al. 2009). Chloroplast changes induced by light variations will affect light utilization (Raven and Geider 2003). In the present study, the large distribution area of *C. meneghiniana*(T) on day 3 cell exhibited an active response to LL. The obvious decrease of $\Delta F/F'_m$ values in the four HLA diatoms at LL which occurred after day 9 illustrated that Chl*a* regulation can help HLA diatoms respond to LL stress effectively. The cell density of HLA at LL on day 3 decreased sharply but recovered quickly from day 3 to 9. The growth curve of HLA diatoms at LL became smooth after day 9 probably due to reduced Chl*a* regulation after day 9. In summary, LL can cause and increase in Chl*a* content and chloroplast volume and a simultaneous shart decrease in the average specific growth rate in HLA diatoms. At the early growth stage, the dramatic increase in Chl*a* content at LL leads to the increase in the α values indicating an enhanced photon-capturing efficiency in HLA diatoms. At the latter growth stage, the Chl*a* content of HLA diatoms at LL decreased sharply together with a decrease in α decrease and a slight decrease in rETR$_{max}$ and I_k.

NPQ regulation

The xanthophyll cycle (XC) dependent non-photochemical quenching (NPQ) is an essential protective mechanism for protecting algae against excess light, which can help dissipate excess energy through thermal radiation (e.g., Krause 1988; Lavaud et al. 2004). The decrease in $\Delta F/F'_m$ of LLA diatoms at HL that began on day 7 or day 9 indicated that NPQ regulation can delay the decline in $\Delta F/F'_m$ although the growth rate

and photosynthesis activity in LLA diatoms at 80 μmol photons m^{-2} s^{-1} was much lower than that at 12.5 and 25 μmol photons m^{-2} s^{-1}. In addition, low growth rates of LLA diatoms in HL might be due to the large energetic cost of the xanthophyll cycle. At the early growth stage of HL treatments, LLA diatoms showed similar characteristics as HLA diatoms with low α and high rETR$_{max}$ and I_k. However, at the latter growth stage when NPQ regulation became weak, the parameters of photosynthesis activity in LLA diatoms decreased. The low Chl*a* content of LLA diatoms at HL before day 7 (except *S. unla*) indicated that Chl*a* regulation also played a regulation role in LLA.

Kashino et al. (2002) pointed that phytoplankton growing on the surface of water column respond to high irradiance more actively than that from a 25 m depth with obviously high NPQ values. High light-adapted species can have a high pool of xanthophyll-cycling pigments per cell compared to low light-adapted species (Dimier et al. 2009). *C. meneghiniana* has a large and flexible NPQ potential because the regulatory components of *C. meneghiniana* (a fast transient component, a steady-state component, and a fast relaxing component) can help *C. meneghiniana* respond to high light fast and effectively (Grouneva et al. 2008; Su et al. 2012). However, there was no significant increase in NPQ values in HLA diatoms under high light, suggesting that the light intensities used were much lower than their saturated value. The higher NPQ values of HLA diatoms observed at LL may relate to the increase in diadinoxanthin (DD). High light-acclimated algae also show high NPQ values in the dark-adapted samples due to a larger DD signal (Serodio et al. 2005). Similar to the HLA diatoms at LL, the NPQ values of LLA diatoms at LL fluctuated around the initial NPQ values on day 1.

The results of the present study confirmed our hypothesis that diatoms had excellent light-adaptive capability to local light conditions and physiological strategies to manage light fluctuation in the short term. The results show that we should consider the photoacclimation of diatoms to their historic light environments when we study the characteristics of certain species and we can potentially use some convenient light control measures to control the dominance of some species in small eutrophic aquatic ecosystems.

References

Anning T, MacIntyre HL, Pratt SM, Sammes PJ, Gibb S, Geider RJ (2000) Photoacclimation in the marine diatom *Skeletonema costatum*. Limnol Oceanogr 45:1807

Barnett A, Méléder V, Blommaert L, Lepetit B, Gaudin P, Vyverman W, Sabbe K, Dupuy C, Lavaud J (2014) Growth form defines physiological photoprotective capacity in intertidal benthic diatoms. ISME J 105:1–14

Behrenfeld MJ, Prasil O, Babin M, Bruyant F (2004) In search of a physiological basis for covariations in light-limited and light-saturated photosynthesis. J Phycol 40:4–25

Bouvy M, Ba N, Ka S, Sane S, Pagano M, Arfi R (2006) Phytoplankton community structure and species assemblage succession in a shallow tropical lake (Lake Guiers, Senegal). Aquat Microb Ecol 45: 147–161

Brunet C, Johnsen G, Lavaud J, Roy S (2011) Pigments and photoacclimation processes. In Phytoplankton pigments, characterization, chemotaxonomy and applications in oceanography. In: Roy S, Johnsen G, Llewellyn C, Skarstad E (eds) Oceanographic methodologies. SCOR-UNESCO Publishing, Cambridge, pp 445–454

Brunet C, Conversano F, Margiotta F, Dimier C, Polimene L, Tramontano F, Saggiomo V (2013) Role of light and photophysiological properties on phytoplankton succession during the spring bloom in the north-western Mediterranean Sea. Adv Oceanogr Limnol 4:1–19

Cheah W, McMinn A, Griffiths FB, Westwood KJ, Wright SW, Clementson LA (2013) Response of phytoplankton photophysiology to varying environmental conditions in the sub-antarctic and polar frontal zone. Plos One 8:e72165

Dauta A, Devaux J, Piquemal F, Boumnich L (1990) Growth rate of four freshwater algae in relation to light and temperature. Hydrobiologia 207:221–226

Dimier C, Giovanni S, Ferdinando T, Brunet C (2009) Comparative ecophysiology of the xanthophyll cycle in six marine phytoplanktonic species. Protist 160:397–411

Edwards GE, Baker NR (1993) Can CO_2 assimilation in maize leaves be predicted accurately from chlorophyll fluorescence analysis? Photosynth Res 37:89–102

Ferris JA, Lehman JT (2007) Interannual variation in diatom bloom dynamics: roles of hydrology, nutrient limitation, sinking, and whole lake manipulation. Water Res 41:2551–2562

Gameiro C, Zwolinski J, Brotas V (2011) Light control on phytoplankton production in a shallow and turbid estuarine system. Hydrobiologia 669:249–263

Genty B, Briantais JM, Baker NR (1989) The relationship between the quantum yield of photosynthetic electron transport and quenching of chlorophyll fluorescence. Biochim Biophys Acta 990:87–92

Gikuma-Njuru P, Guildford SJ, Hecky RE, Kling HJ (2013) Strong spatial differentiation of N and P deficiency, primary productivity and community composition between Nyanza Gulf and Lake Victoria (Kenya, East Africa) and the implications for nutrient management. Freshw Biol 58:2237–2252

Grouneva I, Jakob T, Wilhelm C, Goss R (2008) A new multicomponent NPQ mechanism in the diatom Cyclotella meneghiniana. Plant Cell Physiol 49:1217–1225

Harris G (1978) Photosynthesis, productivity and growth: the physiological ecology of phytoplankton. Schweizerbart, Stuttgart

Hartig JH, Wallen DG (1986) The influence of light and temperature on growth and photosynthesis of Fragilaria crotonensis Kitton. J Freshw Ecol 3:371–382

Hartig P, Wolfstein K, Lippemeier S, Colijn F (1998) Photosynthetic activity of natural microphytobenthos populations measured by fluorescence (PAM) and ^{14}C-tracer methods: a comparison. Mar Ecol Prog Ser 166:53–62

Hijnen WA, Dullemont YJ, Schijven JF, Hanzens-Brouwer AJ, Rosielle M, Medema G (2007) Removal and fate of Cryptosporidium parvum, Clostridium perfringens and small-sized centric diatoms (Stephanodiscus hantzschii) in slow sand filters. Water Res 41: 2151–2162

Hu H, Wei Y (2006) The freshwater algae of China: systematic, taxonomy and ecology. Science Press, Beijing (In Chinese)

Huisman J, Sharples J, Stroom JM, Visser PM, Kardinaal WEA, Verspagen JMH, Sommeijer B (2004) Changes in turbulent mixing shift competition for light between phytoplankton species. Ecology 85:2960–2970

Ihnkena S, Eggertb A, Beardalla J (2010) Exposure times in rapid light curves affect photosynthetic parameters in algae. Aquat Bot 93:185–194

Jaeger CG, Diehl S, Schmidt GM (2008) Influence of water-column depth and mixing on phytoplankton biomass, community composition, and nutrients. Limnol Oceanogr 53:2361–2373

Kashino Y, Kudoh S, Hayashi Y, Suzuki Y, Odate T, Hirawake T, Satoh K, Fukuchi M (2002) Strategies of phytoplankton to perform effective photosynthesis in the North Water. Deep Sea Res II 49:5049–5061

Kim DK, Jeong KS, Whigham PA, Joo GJ (2007) Winter diatom blooms in a regulated river in South Korea: explanations based on evolutionary computation. Freshw Biol 52:2021–2041

Köhler J (1994) Origin and succession of phytoplankton in a river-lake system (Spree, Germany). Hydrobiologia 289:73–83

Kolmakov VI, Gaevskii NA, Ivanova EA, Dubovskaya OP, Gribovskaya IV, Kravchuk ES (2002) Comparative analysis of ecophysiological characteristics of Stephanodiscus hantzschii Grun. in the periods of its bloom in recreational water bodies. Russ J Ecol 33:97–103

Krause GH (1988) Photoinhibition of photosynthesis. An evaluation of damaging and protective mechanisms. Physiol Plant 74:566–574

Kropuenske LR, Mills MM, van Dijken GL, Bailey S, Robinson DH, Welschmeyer NA, Arrigo KR (2009) Photophysiology in two major southern ocean phytoplankton taxa: photoprotection in Phaeocystis antarctica and Fragilariopsis cylindrus. Limnol Oceanogr 54: 1176–1196

Lavaud J, Rousseau B, Etienne AL (2004) General features of photoprotection by energy dissipation in planktonic diatoms (Bacillariophyceae). J Phycol 40:130–137

Laviale M, Prygiel J, Lemoine Y, Courseaux A, Creach A (2009) Stream periphyton photoacclimation response in field conditions: effect of community development and seasonal changes. J Phycol 45:1072–1082

Leland HV, Brown LR, Mueller DK (2001) Distribution of algae in the San Joaquin River, California, in relation to nutrient supply, salinity and other environmental factors. Freshw Biol 46:1139–1167

Letelier RM, Karl DM, Abbott MR, Bidigare RR (2004) Light driven seasonal patterns of chlorophyll and nitrate in the lower euphotic zone of the North Pacific Subtropical Gyre. Limnol Oceanogr 49: 508–519

MacIntyre HL, Kana TM, Anning T, Geider RJ (2002) Photoacclimation of photosynthesis 25 irradiance response curves and photosynthetic pigments 522 in microalgae and cyanobacteria. J Phycol 38:17–38

Marra J, Heinemann K (1982) Photosynthesis response by phytoplankton to sunlight variability. Limnol Oceanogr 27:1141–1153

Migné A, Spilmont N, Davoult D (2004) In situ measurements of benthic primary production during emersion: seasonal variations and annual production in the Bay of Somme (eastern English Channel, France). Cont Shelf Res 24:1437–1449

Pannard A, Bormans M, Lagadeuc Y (2007) Short-term variability in physical forcing in temperate reservoirs: effects on phytoplankton dynamics and sedimentary fluxes. Freshw Biol 52:12–27

Platt T, Gallegos CL, Harrison WG (1980) Photoinhibition of photosynthesis in natural assemblages of marine phytoplankton. J Mar Res 38:687–701

Polimene L, Brunet C, Butenschoen M, Martinez-Vicente V, Widdicombe C, Torres R, Allen JI (2014) Modelling a light-driven phytoplankton succession. J Plankton Res 36:214–229

Qi M, Chen J, Sun X, Deng X, Niu Y, Xie P (2012) Development of models for predicting the predominant taste and odor compounds in Taihu Lake, China. Plos One 7:e51976

Raven JA, Geider RJ (2003) Adaptation, acclimation and regulation in algal photosynthesis. In: Larkum AWD, Douglas SE, Raven JA (eds) Advances in photosynthesis and respiration. Springer, Dordrecht, pp 385–412

Rhee GY, Gotham IJ (1981) The effect of environmental factors on phytoplankton growth: light and the interactions of light with nitrate limitation. Limnol Oceanogr 26:649–659

Robinson CT, Rushforth SR (1987) Effects of physical disturbance and canopy cover on attached diatom community structure in an Idaho stream. Hydrobiologia 154:49–59

Rodríguez P, Pizarro H (2007) Phytoplankton productivity in a highly colored shallow lake of a South American floodplain. Wetlands 27:1153–1160

Rodríguez P, Solange Vera M, Pizarro H (2012) Primary production of phytoplankton and periphyton in two humic lakes of a South American wetland. Limnology 13:281–287

Rothenberger MB, Burkholder JM, Wentworth TR (2009) Use of long-term data and multivariate ordination techniques to identify environmental factors governing estuarine phytoplankton species dynamics. Limnol Oceanogr 54:2107–2127

Schmitt M, Nixdorf B (1999) Spring phytoplankton dynamics in a shallow eutrophic lake. Hydrobiologia 408:269–276

Schreiber U, Bilger W, Neubauer C (1994) Chlorophyll fluorescence as a nonintrusive indicator for rapid assessment of in vivo photosynthesis. In: Schulze ED, Caldwell MM (eds) Ecophysiology of photosynthesis. Springer, Berlin, pp 49–70

Serodio J, Cruz S, Vieira S, Brotas V (2005) Non-photochemical quenching of chlorophyll fluorescence and operation of the xanthophyll cycle in estuarine microphytobenthos. J Exp Mar Biol Ecol 326:157–169

Sokal MA (2007) Assessment of hydroecological changes at the Slave River Delta, NWT, using diatoms in seasonal, inter-annual and paleolimnological experiments. Waterloo, Ontario, Canada

Sommer U (1986) Phytoplankton competition along a gradient of dilution rates. Oecologia 68:503–506

Stamenkovic M, Hanelt D (2013) Adaptation of growth and photosynthesis to certain temperature regimes is an indicator for the geographical distribution of Cosmarium strains (Zygnematophyceae, Streptophyta). Eur J Phycol 48:116–127

Stein JR, Hellebust JA (1979) Handbook of phycological methods: culture methods and growth measurements. Cambridge University Press, Cambridge

Stempak JG, Ward RT (1964) An improved staining method for electron microscopy. J Cell Biol 22:697–701

Su W, Jakob T, Wilhelm C (2012) The impact of nonphotochemical quenching of fluorescence on the photon balance in diatoms under dynamic light conditions. J Phycol 48:336–346

Su M, An W, Yu J, Pan S, Yang M (2014) Importance of underwater light field in selecting phytoplankton morphology in a eutrophic reservoir. Hydrobiologia 724:203–216

Thomas WH, Gibson CH (1990) Effects of small-scale turbulence on microalgae. J Appl Phycol 2:71–78

Tuji A (2000) The effect of irradiance on the growth of different forms of freshwater diatoms: implications for succession in attached diatom communities. J Phycol 36:659–661

van de Poll WH, Visser RJW, Buma AGJ (2007) Acclimation to a dynamic irradiance regime changes excessive irradiance sensitivity of *Emiliania huxleyi* and *Thalassiosira weissflogii*. Limnol Oceanogr 52:1430–1438

van Leeuwe MA, van Sikkelerus B, Gieskes WWC, Stefels J (2005) Taxon-specific differences in photoacclimation to fluctuating irradiance in an Antarctic diatom and a green flagellate. Mar Ecol Prog Ser 288:9–19

Wang Z, Wu W, Zuo M, Li D (2010) Niche analysis of phytoplankton community in Lake Chaohu. Resour Environ Yangtze Basin 19:685–691 (In Chinese)

Wang P, Shen H, Xie P (2012) Can hydrodynamics change phosphorus strategies of diatoms?—nutrient levels and diatom blooms in lotic and lentic ecosystems. Microb Ecol 63:369–382

Wang Y, Deng K, Wang X (2013) Effect of light, nutrient and diatom on the development of *Phaeocystis globosa*. J Ecol Sci 32:165–170 (In Chinese)

Warnaars T, Hondzo M (2006) Small-scale fluid motion mediates growth and nutrient uptake of *Selenastrum capricornutum*. Freshw Biol 51:999–1015

Yang M, Bi Y, Hu J, Hu Z (2011) Diel vertical migration and distribution of phytoplankton during spring blooms in Xiangxi Bay, Three Gorges Reservoir. J Lake Sci 23:375–382 (In Chinese)

Yang Q, Xie P, Shen H, Xu J, Wang P, Zhang B (2012) A novel flushing strategy for diatom bloom prevention in the lower-middle Hanjiang River. Water Res 46:2525–2534

Zeng H, Song L, Yu Z, Chen H (2007) Post-impoundment biomass and composition of phytoplankton in the Yangtze River. Int Rev Hydrobiol 92:267–280

Zhang Z, Huang X (1991) Research methods of freshwater plankton. Science Press, Beijing (In Chinese)

Zhang Y, Qin B, Chen W, Gao G, Chen Y (2004) Experimental study on underwater light intensity and primary productivity caused by variation of total suspended matter. Adv Water Sci 15:615–620 (In Chinese)

Znachor P, Visocka V, Nedoma J, Rychtecky P (2013) Spatial heterogeneity of diatom silicification and growth in a eutrophic reservoir. Freshw Biol 58:1889–1902